UNICA
UNIVERSITÀ
DEGLI STUDI
DI CAGLIARI

A MULTI-SCENARIO APPROACH FOR A ROBUST DESIGN OF SOLAR-BASED ORC SYSTEMS

Mario Petrollese[1]* and Daniele Cocco[2]

[1]University of Cagliari, Department of Mechanical, Chemical and Materials Engineering, Cagliari, Italy
petrollese@unica.it

[2]University of Cagliari, Department of Mechanical, Chemical and Materials Engineering, Cagliari, Italy
daniele.cocco@unica.it

* Corresponding Author

ABSTRACT

The application of Organic Rankine cycle (ORC) units in concentrating solar power systems is a very promising solution. However, fluctuations in the available solar energy often force solar-based ORC systems to operate at part-load conditions. An innovative methodology for finding robust design solutions of such ORC systems, based on the minimization of the expected Levelized Cost of Energy (LCOE), is therefore proposed. The expected variations in the ORC heat source and heat sink are considered during the design stage by adopting a multi-scenario approach. The proposed methodology has been tested by referring to a medium-scale ORC unit and by considering different working fluids. As cases study, the direct coupling of the ORC unit with a solar field and the integration of a Thermal Energy Storage system have been investigated. The comparison of the results obtained by using a multi-scenario and a single-scenario approach highlights a reduction of the actual LCOE. The ORC configuration obtained by adopting a multi-scenario approach is characterized by lower performance under design conditions, but it is less sensitive to variations in the main inputs during off-design operating periods. This fact is particularly noteworthy for the case with the direct coupling of the solar field.

Keywords: Organic Rankine Cycles, concentrating solar power, robust optimization, optimal design, scenario approach

1. INTRODUCTION

Organic Rankine Cycle (ORC) refers to a form of Rankine cycle plant that uses organic substance as working fluid instead of water, basically for the conversion of low-grade heat into useful power. ORC systems can operate efficiently and affordably at lower temperatures and on smaller scales than power systems based on steam-Rankine cycle, making this technology particularly suitable for the recovery of waste heat in industry processes and for the exploitation of renewable energy sources (i.e. solar, geothermal) [1]. However, these heat sources are often characterized by large fluctuations both in terms of mass flow rate and temperature and the ORC unit is usually forced to work at off-design conditions for long operating times [2]. Moreover, because air dry coolers or cooling towers are often used in the condenser water circuit, the variability in the heat sink characteristics due to ambient temperature fluctuations is another source of uncertainty affecting the ORC performance. The flexibility of working at different operating conditions with limited efficiency drops is therefore an important feature requested to ORC units, which should be taken into account even during their design stage [3].
Among the various ORC applications, the adoption of such power systems for the solar-to-electricityconversion is a promising option [4], although the application of ORCs in Concentrating Solar

Power (CSP) plants is still at a demonstration stage and few solar ORC power plants are currently under operation worldwide [5].

The substantial interest in solar-based ORC plants is proven also by the large number of available studies related to the design, analysis and optimization of such systems [6]. One of the main issues concerns the diurnal and seasonal fluctuations of solar irradiation with the consequent request of reliable models for the prediction of the solar-ORC performance in a large range of operating conditions [7]. In this regard, He et al. [8] developed a proper simulation model for analyzing the actual operability of an ORC unit integrated with a solar field in four typical days. Large fluctuations in the mass flow rate of the heat transfer fluid (HTF) circulating in the solar field were detected and their effect on the performance of the whole system were examined. The performance of a 250 kW ORC unit coupled with compound parabolic collectors were investigated by Wang et al. [9] by considering a large range of variation of both ambient temperature and HTF mass flow rate. Significant performance degradation in terms of net power output and average exergy efficiency were found, in particular during the warmer months. The performance under off-design conditions of an ORC unit using n-butane as working fluid and coupled with a solar field was investigated by Calise et al. [10]. Results highlighted the ORC efficiency drop with the increase of heat source mass flow rate and temperature due to the reduction of the pressure difference between boiling and condensing phase. A dynamic model of small-size solar ORC units was developed by Li et al. [11], highlighting the importance of the proper selection of the energy storage capacity to minimize the effects of solar radiation fluctuations and maximize the efficiency. Cioccolanti et al. [12] proposed an innovative small-scale concentrating solar ORC plant coupled with a phase change material storage tank. Results revealed the importance of implementing effective control strategies to face the variation of ambient conditions avoiding high degradation in the plant performance. The effects of the ambient temperature variation on low- and medium-temperature ORC systems were analyzed by Usman et al. [13], and both dry air coolers and cooling tower installed at different geographical locations were considered. An optimization of the ORC design with the objective of maximizing the power output was applied and the operation control strategy was implemented to achieve the maximum power output also with ambient temperatures other than the nominal one. Dickes et al. [14] compared three modelling methods for the ORC off-design simulation, where experimental measurements gathered on two ORC facilities were used as reference for the models' calibration and evaluation.

The important variations in the ORC performance during the off-design conditions as well as their dependence on the design features of the main components were proved and highlighted by the previous studies. For this reason, the proper characterization of the heat source and heat sink, including their expected variation, could be beneficial even during the ORC design process, leading to more robust design solutions able to achieve better performance during the overall plant lifetime. Obviously, a robust design is obtainable if the uncertain input parameters can be characterized and their variability is predictable in a certain way. This approach could be applicable to solar ORC systems, since the annual availability of solar energy for a given location as well as its daily and seasonal variability can be statistically predicted by several forecast models [15]. However, the robust optimization of ORC units under variable input parameters is quite elusive in the state of the art and often it is not directly related to solar applications. Among the few studies available in literature, a thermo-economic optimization of a solar-based ORC plant was proposed by Hajabdollahi et al. [16], where the main design parameters (evaporator and condenser pressures, working fluid mass flow rate and regenerator effectiveness) were optimized to maximize the relative annual benefit by considering the hourly system performance. Mavrou et al. [17] proposed a systematic sensitivity procedure considering the impacts of working fluid and ORC design/operating decisions on the ability of the ORC unit to face operating conditions different from the nominal one. A robust optimization approach for the waste heat recovery of heavy-duty engines was proposed by Bufi et al. [18], where the fluctuations of exhaust gas mass flow rate and temperature were evaluated. A two-step optimization methodology for the design and off-design optimization of geothermal ORC units was proposed by Van Erdeweghe et al. [19], where the off-design performance were calculated for evaluating the expected net present value. Pili et al [20] developed an integral optimization code based on 8 optimization variables, where both design and off-design performance were evaluated to minimize the expected cost of energy of an ORC unit using the waste heat produced by a billet reheating furnace.

In this framework, a novel methodology for the preliminary design of an ORC unit operating under variable conditions has been recently proposed by the authors [21]. A multi-scenarios approach has been used to simulate the expected variability of the heat source and heat sink during the ORC operating time. Each scenario represents the probability of occurrence of given class range values of the selected design variables. The generated scenarios have been involved in an optimization process of the main design cycle variables with the objective of minimizing the expected levelized cost of energy (LCOE). In this paper, the capabilities and the benefits of the aforementioned method for the design of medium-scale solar-based ORC units are investigated by considering different heat source and heat sink characteristics as well as different working fluids. As case study, the direct coupling of the ORC unit with a solar field is investigated. Furthermore, the introduction of a thermal energy storage system, with the consequent reduction in fluctuations of the heat source mass flow rate, is also examined. In all the cases, the results obtained by using a multi-scenario approach are compared with those obtained by a single-scenario approach. The main aims of the study are:

- to assess the potential benefits in using a multi-scenario approach for the design of solar-based ORC units under different boundary conditions and to test the robustness of the optimized solutions;
- to analyze the influence of the working fluid in the design of ORC units by using a multi-scenario approach;
- to investigate the effect of the number of scenarios on the optimal ORC design process.

The remainder of this paper is organized as follows: the details of the methodology are reported in section 2, the definition of the case studies analyzed is reported in section 3, the main results are shown and discussed in section 4 and the main findings are summarized in section 5.

2. METHODOLOGY

The proposed methodology used for the preliminary design of an ORC unit considering the expected fluctuations in the heat source and heat sink characteristics is schematically shown in Figure 1. The design procedure starts with some general assumptions, such as the choice of the working fluid (with the corresponding evaluation of the thermodynamics properties) and the general layout of the ORC unit. The following step concerns the proper characterization of the heat source (the HTF mass flow rate is taken as reference in this analysis) and heat sink (ambient temperature) by means of a scenarios generation. Starting from the expected variability of these inputs during a given reference period (one year in this study), a specified number of scenarios (n_s) with a certain probability of occurrence (p_s) is defined through the class discretization of the frequency distribution of the given parameter. Consequently, each scenario is described by the mean value of the represented class range and the corresponding probability of occurrence. The latter is calculated as the ratio between the frequency (in hours) of the class and the overall operating hours of the ORC unit.
Subsequently, an optimization procedure is implemented for the identification of the ORC design achieving the minimum expected LCOE. In this case, five independent design variables are optimized, namely, condensing temperature (T_{CD}, directly related to the minimum cycle pressure), evaporating temperature (T_{EV}, directly related to the maximum cycle pressure), degree of superheating (ΔT_{SH}, that is the difference between the maximum cycle temperature and the evaporator saturation temperature), recuperator effectiveness (ε_{REC}) and working fluid mass flow rate ($\dot{m}_{WF}$). Obviously, the method could include other variables. Because of the non-linearity of the mathematical problem, a genetic algorithm was used to find the optimum solution. For the case presented here, an initial population of 100 individuals was built inside the range of variability defined by the lower and upper bounds of each variable. It is noteworthy to observe that the algorithm stops if the average relative change in the best fitness function over the 50^{th} generation is less than 0.1%. For each individual of the population (which represents a possible ORC configuration), the expected LCOE is calculated according to three steps.

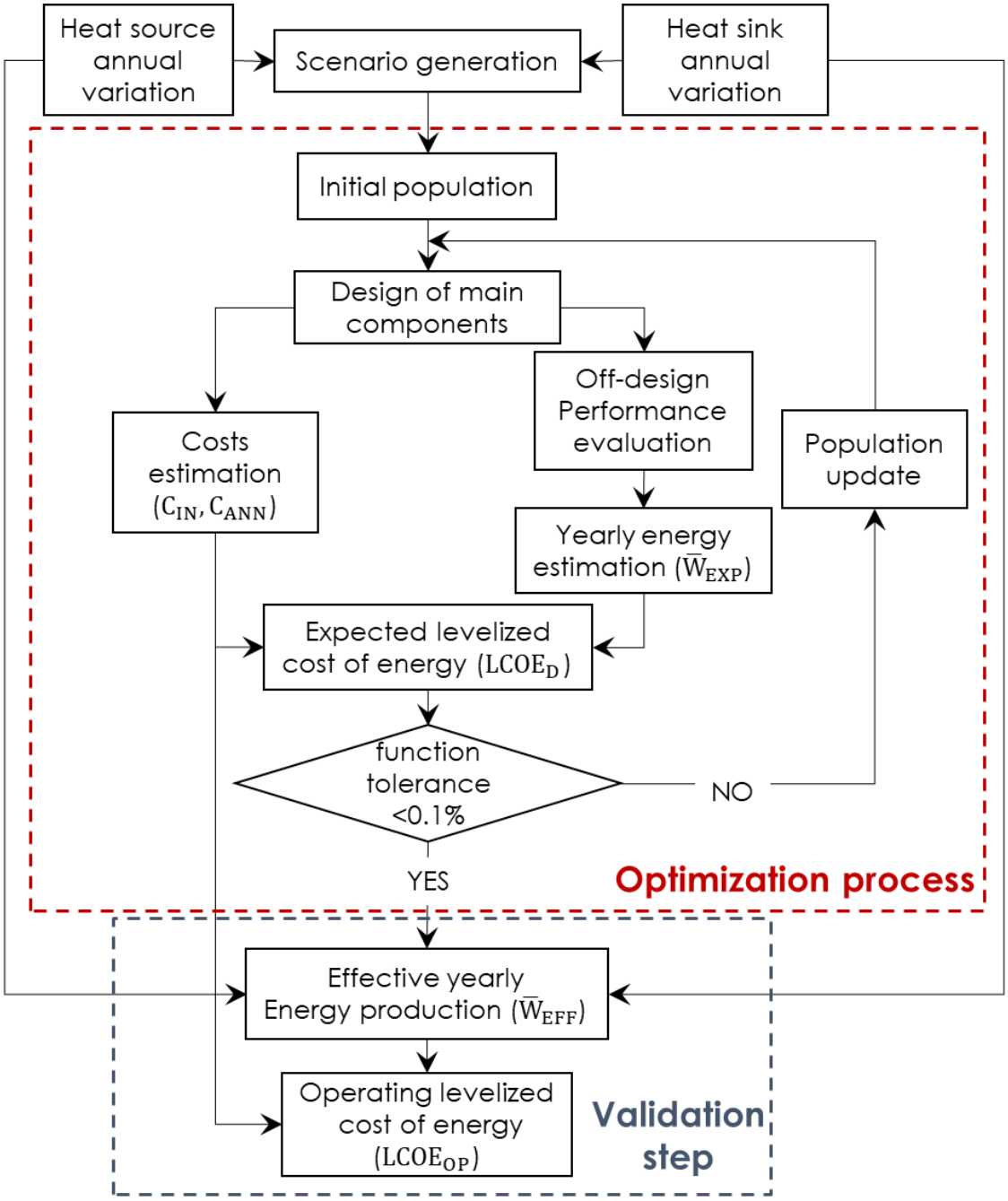

Figure 1 - Schematic procedure adopted for the preliminary design of a solar-based ORC unit.

The first step corresponds to the design stage of the ORC unit, where the thermodynamic cycle under design conditions is defined according to the five independent variables, the preliminary design of the main components, (heat exchangers area and turbomachinery size) is carried out and investment and annual costs of the ORC unit are estimated. The second step concerns the assessment of the ORC performance under off-design conditions. By considering the ORC unit designed in the previous step, its expected performance is calculated for each scenario considered and, accordingly, the annual energy produced by the ORC unit is evaluated starting from the corresponding probabilities of occurrence. Finally, the expected levelized cost of energy of the ORC unit, that is the objective function of the optimization problem, is evaluated.

As formulated, the optimization problem requires the development of proper ORC models for the design of the main components and for the evaluation of the ORC performance at off-design conditions. The thermodynamic cycle under the design conditions is completely defined by the five variables to be

optimized (a subcritical recuperative cycle is assumed). The operating conditions are rearranged during off-design conditions in order to maximize the mass flow rate of the working fluid (and thus the net power produced by the ORC unit) based on the main component performance. The fluid properties are calculated by using the Coolprop database [22].

All the heat exchangers (preheater, evaporator, recuperator and condenser) of the ORC under investigation are shell and tube type, with single shell and double tube pass in E configuration. By introducing a minimum value for the temperature differences inside the heat exchangers (5°C) as a constraint and with the assumption of negligible heat losses, since both the inlet and outlet temperatures of all the heat exchangers are known during the design-stage, the LMTD method is used for the evaluation of their overall heat exchange area A:

$$\dot{Q} = U \cdot A \cdot LMTD \tag{1}$$

where U is the overall heat transfer coefficient and LMTD indicates the log mean temperature difference. The overall heat transfer coefficient is evaluated by assuming negligible fouling and thermal conductive resistance, namely, by considering only the convective heat transfer coefficients on the tube side and the shell side. The latter were evaluated by using specific models proposed in previous studies [10,23,24]. The same correlations are used for the estimation of the overall heat transfer coefficient during off-design operation, while the ε-NTU method is adopted for the evaluation of the performance of heat exchangers.

An axial turbine and a centrifugal pump coupled with a variable frequency drive are selected as turbomachines. The power produced by the turbine ($\dot{W}_T$) is calculated as follows:

$$\dot{W}_T = \dot{m}_{WF}\, \Delta h_T\, \eta_T\, \eta_{EM,T} \tag{2}$$

where $\dot{m}_{WF}$ is the working fluid mass flow rate, Δh_T is the specific enthalpy change of the working fluid, η_T is the turbine isentropic efficiency and $\eta_{EM,T}$ is the electric generator efficiency including the gearbox efficiency (imposed equal to 0.88 in this analysis). At design conditions, the isentropic efficiency and the number of stages are calculated according to the correlations proposed by Astolfi e Macchi [25], as a function of the size parameter and the volume ratio, while the specific speed was optimized for each case. At off-design conditions, the turbine isentropic efficiency is calculated as a function of the volumetric flow ratio. According to Gabbrielli [26], the turbine operates in a sliding pressure mode, with a fixed nozzle area and the Stodola's ellipse approach is used to evaluate the turbine inlet pressure. To avoid liquid presence at the turbine inlet, the complete evaporation of the working fluid in the evaporator is assumed, while the partial evaporation of the pressurized liquid in the recuperator is not permitted.

The power required by the pump ($\dot{W}_P$) is calculated as follows:

$$\dot{W}_P = \frac{\dot{m}_{WF}\, \Delta h_P}{\eta_P\, \eta_{EM,P}} \tag{3}$$

where Δh_P is the specific enthalpy change of the working fluid, η_P is the pump isentropic efficiency and $\eta_{EM,P}$ denotes the electric motor efficiency including the gearbox efficiency. Owing to the low effect of the pump power on the ORC power output, constant values for both the pump isentropic efficiency and the electromechanical efficiency are assumed (0.8 and 0.86, respectively).

Air dry coolers are used in the cooling water circuit and, starting from the ambient temperature, the cooling water inlet temperature is calculated by assuming an approach temperature of 10 °C. The difference between the inlet and the outlet temperatures of the condenser cooling water is assumed equal to 15°C and the cooling water mass flow rate is calculated to assure the complete condensation of the working fluid stream. The energy production of the ORC unit is given by the product of the ORC power output (that is the difference between the power produced by the turbine and that required by the pump) and the corresponding operating time.

The overall investment cost of each ORC solution depends on the heat transfer area of preheater/evaporator (A_{EV}), recuperator (A_{REC}) and condenser (A_{CD}), together with the nominal power

of both turbine ($\dot{W}_T$) and pump ($\dot{W}_P$). Therefore, the investment cost C_{IN} is calculated as the sum of the bare module costs, that are the product of the purchased equipment cost (C_p^0) and the bare module factor (F_{BM}) of the five main ORC components, in accordance with the approach proposed by Turton et al. [27], while the annual operating costs (C_{ANN}) are assumed equal to 2% of the overall investment cost.
For each solution, the expected yearly ORC net energy production ($\overline{W}_{EXP}$) is computed as the product of the expected annual operating time (t_{OP}) and the weighted mean value of the net ORC power estimated in each scenario, being the weights the probabilities of occurrences (p_s) of the various scenarios:

$$\overline{W}_{EXP} = t_{OP} \cdot \sum_{s=1}^{n_S} p_s \cdot \dot{W}_{NET}(s) \tag{4}$$

The estimation of the LCOE during the design of the ORC unit (called design LCOE - $LCOE_D$) is therefore computed by using the following correlation:

$$LCOE_D = \frac{C_{IN} + \sum_{n=1}^{N} \frac{C_{ANN}}{(1+i)^n}}{\sum_{n=1}^{N} \frac{\overline{W}_{EXP}}{(1+i)^n}} \tag{5}$$

where i is the discount rate (set equal to 7%) and N is the expected plant lifetime (assumed equal to 20 years). It is worth noting that the overall costs for the calculation of the expected LCOE directly depend on the design cycle, while the expected net energy production depends on the behavior of the system during operating periods, including off-design operations.
Once the design of the ORC unit is completed and the system configuration is optimized according to the scenarios considered, the actual performance of the ORC unit are computed by simulating the yearly operation of the ORC unit, namely, by taking into account the hourly fluctuations of the HTF mass flow rate and ambient temperature. In this way, the effective yearly ORC net energy production ($\overline{W}_{EFF}$) can be calculated as:

$$\overline{W}_{EFF} = \sum_{t=1}^{8760} \dot{W}_{NET}(t) \cdot \Delta t \tag{6}$$

where Δt is the time step, imposed equal to 1 hour. Consequently, the effective LCOE occurring during the operating phase of the ORC unit (called operating LCOE – $LCOE_{OP}$) can be calculated by substituting in eq. (5) the expected yearly energy production, $\overline{W}_{EXP}$, with the effective yearly energy production, $\overline{W}_{EFF}$.

3. CASE STUDY

The methodology described in the previous section is applied to the design of an ORC unit integrated in a medium-size CSP plant. The configuration of an existing CSP-ORC plant (Ottana solar facility) is used as reference for the definition of the heat source and heat sink characteristics [5]. In particular, the heat source of the ORC unit consists of a solar field based on linear Fresnel collectors and, in case, a two-tank direct TES system, while the heat sink is based on dry coolers.
The meteorological data set obtained from the Meteonorm software for the location of Ottana (Italy) is used as main input since the characteristics of the heat source and heat sink of the ORC unit mainly depend on the solar irradiance and ambient temperature, respectively. Starting from these meteorological data, the expected solar field performance during a typical year of operation are computed according to the mathematical model presented in [28]. In particular, the thermal power output of the solar field is evaluated as the difference between the thermal power concentrated on the receiver tube and the sum of the optical losses of the collector and the thermal losses in the receiver and in the piping. The receiver power is calculated according to the collecting area, the reference optical efficiency, the longitudinal and transversal components of the Incidence Angle Modifier (IAM), the end-loss optical efficiency and the mirror cleanliness factor. Thermal losses in the receiver and in the

piping are evaluated in function of the difference between the average oil temperature and ambient temperature. For the case here considered, the hourly mass flow rate circulating in a single collector (characterized by a net collecting area of 1430 m^2) is calculated by assuming a thermal oil (Therminol SP-I) as HTF, which is heated up from its inlet temperature (165°C) to the design outlet temperature (275 °C). Figure 2 shows the expected annual trend of the HTF mass flow rate circulating in the single solar collector.

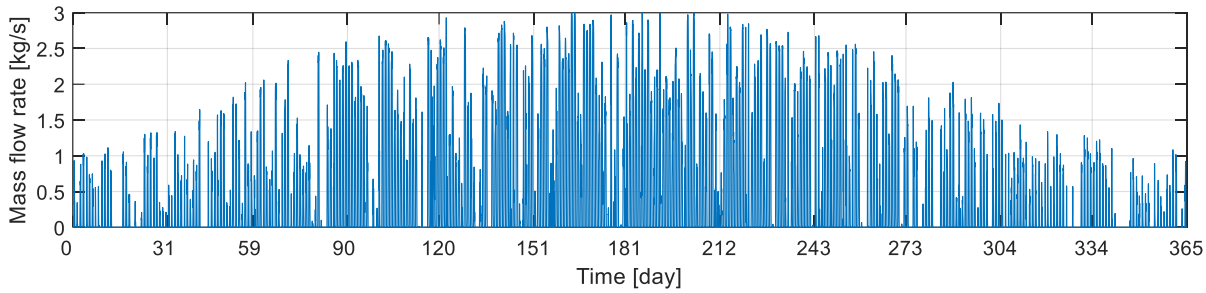

Figure 2 – Expected HTF mass flow rate produced by a collector line.

The overall HTF mass flow rate feeding the ORC unit ($\dot{m}_{HTF}$) is consequently determined based on the HTF mass flow rate circulating in the single collector and it depends on the imposed solar multiple (which is representative of the overall number of collectors) and the storage capacity of the TES system (if present). In this paper, four cases study are analyzed. In the first two cases, the direct coupling of the ORC unit with the aforementioned solar field is investigated, without any TES system. Consequently, the ORC unit is frequently fed by HTF mass flow rates far from the nominal one (12 kg/s) due to the large variability of solar radiation. In the first case study (Case #1), the solar field is designed to produce a nominal HTF mass flow rate equal to 12 kg/s, which corresponds to that required by the ORC unit under nominal conditions. A solar multiple (SM) equal to 1 is therefore imposed and the solar field is composed of 4 collector lines. The second case study (Case #2) is based on 6 collectors (which means a SM=1.5) and the maximum HTF mass flow rate circulating in the solar field is therefore equal to 18 kg/s. The latter is taken as reference case since the solar field configuration corresponds to that of the Ottana solar facility. Obviously, without a TES section, since the HTF mass flow rate circulating in the solar field cannot exceed that required by the ORC, a proper number of collector lines are often defocused, leading to the so called defocusing energy losses. In particular, without a TES section, the defocusing losses occurs if the HTF mass flow rate produced by the solar field exceeds 12 kg/s.
Therefore, to avoid these defocusing losses, as well as to reduce the operating time in which the ORC works at off-design conditions, the inclusion of a two-tank direct TES system is also analyzed. The simulation model of the TES section is based on the energy and mass balances for the two oil tanks by assuming a constant tank temperature and negligible heat losses. Two different storage capacities (h_{TES}), namely, 2.5 and 5 equivalent hours of ORC operation under nominal conditions, are considered. In these cases (Case #3 and Case #4, respectively), the TES system stores the thermal energy produced by the solar field until the hot tank reaches the 50% of its overall storage capacity, after that the start-up of the ORC unit occurs. It should be observed that Case #4 corresponds to the TES section of the Ottana solar facility. The design configurations of the four cases are summarized in Table 1.

Table 1 – Main characteristics of the solar field and TES section assumed for the four case studies.

Case	**Solar multiple (SM)**	**Collector lines**	**Storage capacity** (h_{TES})
#1	1	4	-
#2	1.5	6	-
#3	1.5	6	2.5 h
#4	1.5	6	5 h

For the four aforementioned cases, Figure 3(a) shows the cumulative frequency distribution of the hourly HTF mass flow rate feeding the ORC unit. As expected, the largest variability in the HTF mass flow rate feeding the ORC unit is obtained for Case #1, where the ORC unit very frequently operates under off-design conditions due to a reduced HTF mass flow rate. Furthermore, as shown in Figure 3(b), almost 5% of the annual thermal energy the solar field could potentially produce is lost through a mirror defocusing. In this case, the defocusing losses refer to the operating time when the solar field could produce a thermal power output lower than the minimum input imposed for the ORC unit (20% of the nominal thermal input). The ORC operates at part-load conditions for almost 75% of the operating time also in the reference case (Case #2), where the direct coupling with a solar field designed for a solar multiple of 1.5 is investigated. As shown by Figure 3(b), the maximum percentage of defocusing losses occurs in this case due to the operating time when the solar field could produce a thermal power output higher than the ORC nominal thermal input. The introduction of a storage system (Case #3 and Case #4) leads to an important increase of the ORC operating hours at nominal HTF mass flow rate, reaching almost 90% of occurrence for the case h_{TES}=5 h, as well as to an important reduction in the defocusing losses.

The frequency distribution of Figure 3(a) is used for the scenario's generation step in the proposed design methodology. Figure 4(a-b) shows the main features of the generated scenarios in terms of mean class value and corresponding percentage of occurrence for the five cases.

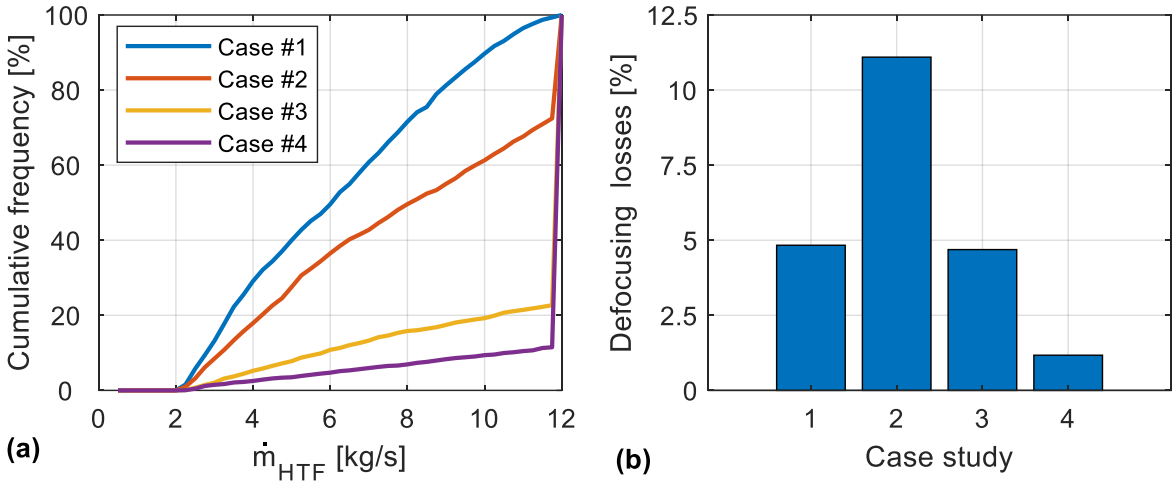

Figure 3 – (a) Cumulative frequency distribution of the annual HTF mass flow rate feeding the ORC unit and (b) percentage of potential solar field thermal production lost by mirror defocusing.

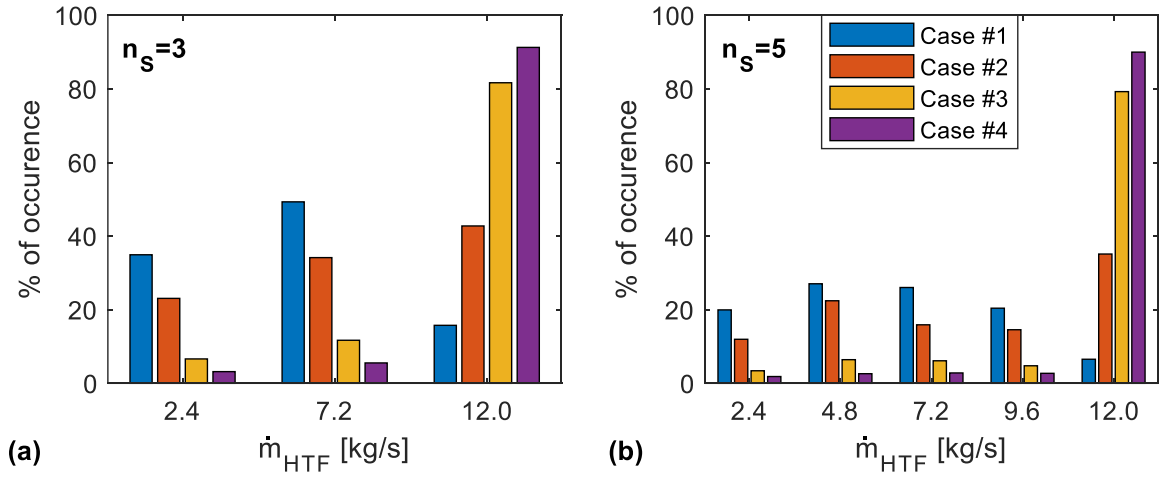

Figure 4 – (a) Yearly percentage of occurrence of the HTF mass flow rate feeding the ORC unit by assuming 3 scenarios and (b) 5 scenarios.

With n_S=3 (Figure 4(a)), the HTF mass flow rate variation is described by a main scenario where the ORC operates with the nominal mass flow rate, a second scenario where the HTF mass flow rate is 60% of the nominal one and a third scenario where the minimum HTF mass flow rate is considered (20% of the nominal one). Obviously, the probability of occurrence of the first scenario increases with the solar multiple and with the storage capacity. The introduction of five scenarios (Figure 4(b)), with a consequent decrease of the class range, results in a more detailed frequency distribution.
Together with the variation in the heat source mass flow rate, the change in the ambient temperature determines some effects on the ORC performance, especially if dry air coolers or, to a lesser extent, cooling towers, are used in the cooling water circuit. This is due to the influence of this parameter on the ORC condenser temperature, and thus on the cycle performance. Although this effect is of minor importance compared to that of the heat source mass flow rate variation, the expected changes of the ambient temperature during the ORC operation could be introduced through the definition of proper scenarios. In particular, Figure 5(a) shows the cumulative frequency distribution of the ambient temperature during the operating hours of the ORC unit. The ORC unit operates from 0 °C to 35 °C, with most of the operating hours in the range from 10 °C to 27.5 °C. The ambient temperature variation is introduced in the proposed methodology by generating 3 additional scenarios, as shown in Figure 5(b). Starting from the ambient temperature, the cooling water inlet temperature was calculated by assuming an approach temperature of 10 °C in the dry air cooler.

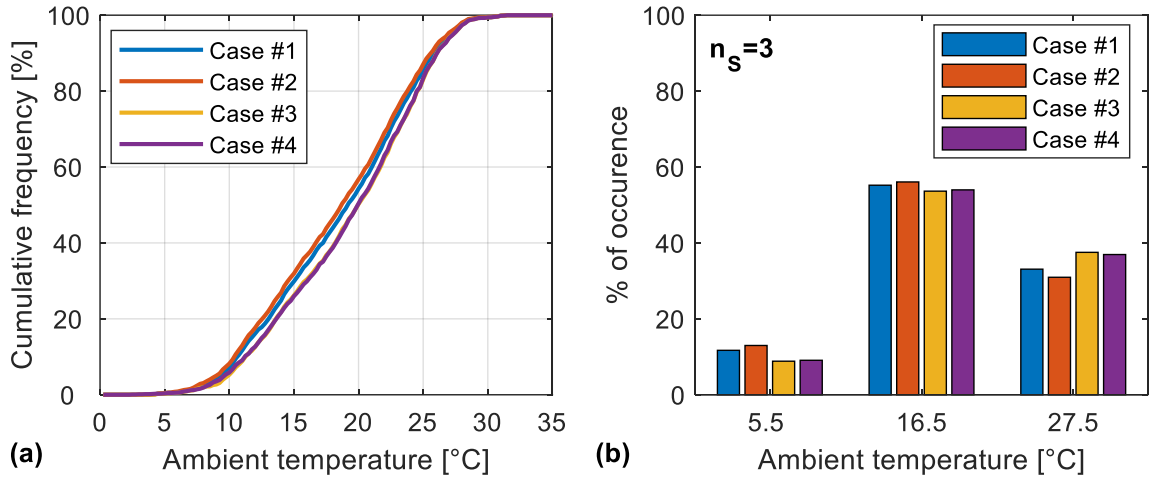

Figure 5 - (a) Cumulative frequency distribution of the ambient temperature during the ORC operating time and (b) corresponding scenarios and percentage of occurrence assumed.

4. RESULTS AND DISCUSSION

Starting from the characteristics of the solar field and the TES section discussed in the previous section, the results obtained by the design of an ORC unit based on a multi-scenarios approach including 3, 5 (that is by considering the sole HTF mass flow rate variation) and 9 scenarios (which includes also the ambient temperature variation) are analyzed. The obtained results are compared to those obtained by the single-scenario approach, where the HTF mass flow is set equal to the design one and the yearly average ambient temperature is considered for characterizing the heat sink (obviously, different heat source/sink characteristics could be assumed, such as the average heat source availability or the minimum heat sink temperature, leading to different ORC unit designs). Five different organic fluids (benzene, cyclopentane, MM, octane and toluene) are considered as possible working fluids since they are characterized by a thermodynamic behavior suitable to ensure a dry expansion.
By referring to the reference case study (Case #2, solar multiple of 1.5 without the presence of the TES section), Table 2 reports the optimized five variables achieved at the end of the optimization procedure, together with the corresponding "design" LCOE ($LCOE_D$, that is the value of the objective function calculated during the design phase) and the "operating" LCOE ($LCOE_{OP}$), which is here assumed as representative of the effective LCOE achieved during the operating phase of the ORC unit. Moreover,

for comparative purposes, the main design parameters in terms of heat exchange areas, design net power output and capital costs are reported in Table 3, together with the expected and the effective yearly net energy productions ($\overline{W}_{EXP}$ and $\overline{W}_{EFF}$, respectively). The main differences between the ORC unit designed by using the multi-scenarios approach and that achieved by using the single-scenario one is the increase of the maximum cycle temperature, in particular the degree of superheating, with the consequent increase of the heat transfer area of the working fluid heating sections (preheater, evaporator and superheater). This outcome together with the slight reduction in the working fluid mass flow rate is common to all the working fluids analyzed and allows to achieve a more robust design. In fact, the introduction of a superheating section is not usual for ORC units, since the benefits in terms of efficiency improvement are marginal compared to the increment in the initial costs. However, the inclusion of a superheating section is proposed by the multi-scenario approach since it leads to ORC units less sensitive to the variation of the boundary conditions and, thus, characterized by lower performance drop during part-load operations.

By way of example, Figure 6 shows the variation of the ORC net power production as a function of the HTF mass flow rate by using Toluene for the case with 3 scenarios, compared to that obtained for the single scenario case. As can be observed, although at nominal conditions ($\dot{m}_{HTF}$=12 kg/s) the difference of the net power output is less than 10 kW, during part-load operations the ORC unit designed with the multi-scenario approach is able to produce up to 15% more power than that obtained with the single scenario approach.

With the multi-scenario approach, the minimization of the condensing temperature is always pursued. In particular, a slight decrease of both condenser temperature (Table 2) and condenser heat transfer area (Table 3) is observed for the multi-scenario approach thanks to the decrease in the working fluid mass flow rate. This fact leads to a higher turbine enthalpy drop and therefore to a higher specific useful work.

In case of regenerative cycles (chosen by the optimization tool only for MM and Octane, because the use of other working fluids leads to a higher specific work and a lower thermal power available at the turbine discharge), a reduction of the recuperator effectiveness is also found by using the multi-scenarios approach, with the consequent reduction of the recuperator heat transfer area. It is worthy to mention the case of the Octane, where the inclusion of scenarios involving ambient temperature variations leads to the choice of a non-regenerative cycle, unlike the other cases where a recuperator downstream the expander is always included.

Apart from the latter case, minor variations in the initial costs are observed by varying the number of considered scenarios, while the main discrepancies between the adoption of a single or a multi-scenario approach occur for the calculation of the expected yearly energy production. In fact, the single scenario approach assumes that the ORC unit operates always under design conditions and therefore, as reported in Table 3, the expected yearly energy production reaches its maximum value. Since the initial and annual costs are almost constant for a given working fluid, the design LCOE achieves the minimum value for the single scenario approach. On the other hand, the reduced HTF mass flow rates considered by the multi-scenario approach lead to lower values of $\overline{W}_{EXP}$ with the consequent increase of the $LCOE_D$ calculated during the design stage.

As expected, the operating LCOE reported in Table 2, which is calculated by considering the actual operating conditions of the ORC unit during one year of operation for the five working fluids and the different scenarios, is higher than the design LCOE. However, the adoption of the multi-scenarios approach results in a design solution able to achieve lower values of the $LCOE_{OP}$ as well as lower differences between the $LCOE_D$ and the $LCOE_{OP}$ in comparison with the single scenario approach. This fact is observed for all the working fluids, with a general reduction of the LCOE in the order of 3-5%. The increase of the number of scenarios always leads to a reduction of the operating LCOE, although the marginal benefits become more and more negligible. A higher number of scenarios also leads to a lower difference between the expected and the effective net energy production, owing to the more detailed characterization of the expected operating conditions the ORC unit even during the design stage.

Table 2 - Optimal ORC design for five different working fluids by adopting the single and the multi-scenarios design methodology.

Working Fluid	$\mathbf{n_s}$	$\mathbf{T_{CD}}$ [°C]	$\mathbf{T_{EV}}$ [°C]	$\mathbf{\Delta T_{SH}}$ [°C]	$\mathbf{\varepsilon_{REC}}$ [-]	$\mathbf{\dot{m}_{WF}}$ [kg/s]	$\mathbf{LCOE_D}$ [€/MWh]	$\mathbf{LCOE_{OP}}$ [€/MWh]
Benzene	1	48.8	220.4	1.0	-	5.6	90.9	134.4
	3	47.9	216.5	15.3	-	5.3	126.7	134.3
	5	47.7	209.2	25.3	-	5.2	124.9	133.1
	9	48.3	212.0	19.4	-	5.3	129.7	131.5
Cyclopentane	1	47.8	202.7	10.7	-	5.7	97.9	144.0
	3	46.5	201.0	27.8	-	5.3	137.8	141.0
	5	45.8	221.2	28.9	-	5.1	131.4	139.7
	9	45.7	220.1	30.0	-	5.1	135.8	138.9
MM	1	47.2	210.4	24.1	0.78	9.8	104.8	149.1
	3	46.0	219.7	30.0	0.68	8.9	145.1	147.8
	5	45.8	216.8	29.9	0.65	8.8	143.7	147.8
	9	45.9	218.0	29.9	0.67	8.8	149.1	147.8
Octane	1	49.7	225.1	3.6	0.67	6.3	98.6	145.4
	3	47.3	216.8	20.4	0.62	5.9	137.7	143.1
	5	47.0	216.6	20.6	0.62	5.9	136.8	143.1
	9	44.6	226.1	17.6	-	4.6	138.4	142.7
Toluene	1	49.4	201.1	6.4	-	5.6	91.1	134.7
	3	47.4	207.0	28.1	-	5.2	126.4	131.7
	5	47.4	207.0	27.6	-	5.2	124.5	131.4
	9	46.4	213.8	12.2	-	5.3	129.0	131.3

Table 3 – Main ORC design characteristics, initial costs, expected and effective yearly net energy production by adopting the single and the multi-scenarios design methodology.

Working Fluid	$\mathbf{n_s}$	$\mathbf{A_{CD}}$ [m^2]	$\mathbf{A_{REG}}$ [m^2]	$\mathbf{A_{EV}}$ [m^2]	$\mathbf{\dot{W}_{NET}}$ [kW]	$\mathbf{C_{IN}}$ [M€]	$\mathbf{\overline{W}_{EXP}}$ [MWh]	$\mathbf{\overline{W}_{EFF}}$ [MWh]
Benzene	1	252.2	-	149.2	696.1	1.36	1.72	1.16
	3	228.2	-	174,1	679.6	1.36	1.23	1.16
	5	218.6	-	184.5	672.9	1.35	1.23	1.16
	9	222.4	-	174.7	675.5	1.35	1.19	1.18
Cyclopentane	1	275.5	-	135.1	612.2	1.32	1.55	1.05
	3	251.6	-	166.7	618.7	1.33	1.1	1.08
	5	242.3	-	263.8	639.3	1.39	1.21	1.14
	9	241.3	-	264.3	637.7	1.39	1.17	1.14
MM	1	251.1	363.4	250.9	698.6	1.59	1.73	1.22
	3	218.1	232.9	321.8	672.9	1.55	1.22	1.2
	5	214.6	211.4	291.2	660.2	1.52	1.21	1.18
	9	206.1	177.0	336.5	644.0	1.50	1.15	1.16
Octane	1	182.8	209.4	191.7	709.3	1.52	1.77	1.20
	3	174.2	168.2	220.6	698.7	1.51	1.25	1.21
	5	174.7	167.1	219.4	698.1	1.51	1.26	1.21
	9	127.5	-	222.9	563.1	1.26	1.04	1.01
Toluene	1	175.7	-	123.4	645.9	1.30	1.63	1.10
	3	158.3	-	182.1	660.3	1.32	1.26	1.15
	5	157.2	-	182.2	660.6	1.32	1.20	1.15
	9	171.3	-	156.0	674.7	1.33	1.18	1.16

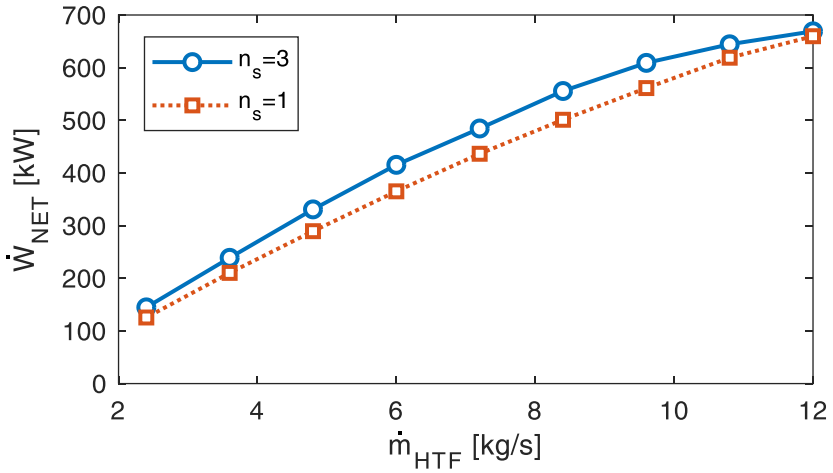

Figure 6 – Variation of the ORC power with the HTF mass flow rate using Toluene**.**

In other words, regardless the working fluid, the design solutions proposed by the multi-scenarios approach are characterized by a design LCOE higher than that proposed by the single scenario (where only design conditions are considered) but less sensitive to the variation of the main inputs. This fact is shown in Figure 7, where, starting from the design LCOE obtained for a case when the ORC would operate always at nominal conditions (blue bars), the negative effects due to reduced mass flow rate (red bars) and ambient temperature fluctuations (green bars) are introduced to determine the operating LCOE. As shown by Figure 7, an increase in the LCOE by considering only nominal conditions (blue bars) is observed with the rise in the number of scenarios even if a lower performance drop is obtained during the ORC part-load operation, with a consequent increase of the annual energy produced by the unit and a corresponding lower final LCOE. The Cyclopentane case well explains this behavior: the solution proposed by the multi-scenarios approach with n_s=9 is characterized by an LCOE at nominal conditions 15% higher than that obtained by the single scenario approach. However, this design solution is less sensitive to the HTF mass flow rate variation and its performance are not influenced by the temperature variation. Accordingly, the operating LCOE is 5% lower than that with n_s=1. Finally, it is worth noting that the best solution (that is the solution with minimum operating LCOE) is obtained using Toluene as working fluid, unlike the case of the single-scenario approach, where Benzene reaches the minimum design LCOE. This result demonstrates the potential benefits in involving a multi-scenario approach even during the selection of the most appropriate working fluid to be used in case the ORC unit operates under variable boundary conditions.

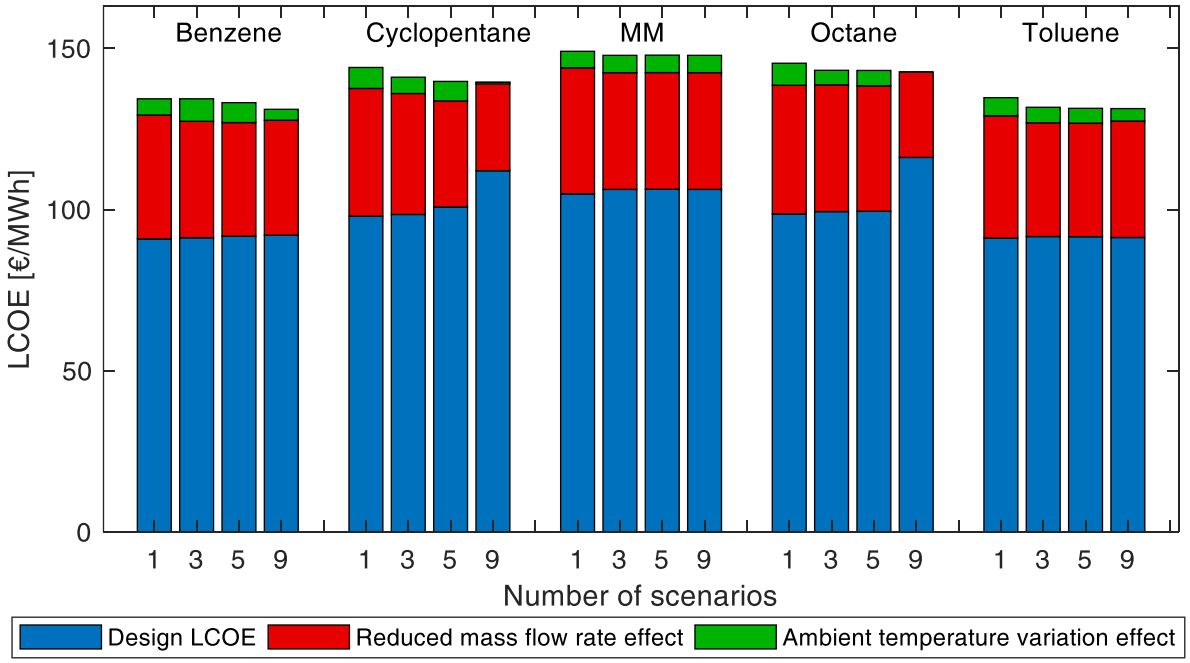

Figure 7 – Levelized cost of energy obtained for the five working fluids**.**

4.1 Influence of the solar field and TES configuration

As mentioned, the configuration of the thermal energy production and storage sections strongly influences the characteristics of the heat source available for the ORC unit. For instance, the inclusion of a TES section reduces the HTF mass flow rate fluctuations and leads to an increase of the ORC operating hours at nominal conditions. Therefore, an improvement of the ORC performance is obtained with a consequent increase of both the average conversion efficiency and the annual energy production, with a corresponding decrease of the levelized cost of energy. On the other hand, the reduction of the solar multiple increases the period when the ORC unit operates with a reduced HTF mass flow, with a consequent reduction of the average conversion efficiency. Accordingly, in this section, the effect of the heat source characteristics on the multi-scenario approach design procedure is investigated.

In particular, the multi-scenario and the single-scenario approaches for the design of a solar ORC unit is tested and compared with reference to the four cases presented in Section 3. Table 4 reports the optimal design solution found for the four cases as a function of the number of scenarios considered during the optimization process by using Toluene as working fluid (that is the organic fluid with the lowest LCOE in the previous section). As observed, a decrease of the superheating degree and a simultaneous increase of the evaporator temperature are proposed as optimal design solutions by the multi-scenario approach in comparison with the single-scenario one for the no-TES cases (Case #1 and Case #2). This leads to an increase of the nominal net power output of the ORC unit, which can be exploited for a longer operating time, allowing to offset the corresponding increase of the ORC initial costs. This fact is particularly evident for the case with nine scenarios where the ambient temperature variation is involved in the optimization process. Minor variations in the optimal design variables are detected by comparing Case #1 with Case #2, even if the latter case is characterized by a lower difference between design and operating LCOE values. Moreover, Case #1 achieves more benefits from the multi-scenario approach than Case #2 due to the longer off-design operating periods.

The inclusion of a TES section (Case #3 and Case #4) leads to a decrease in both the design and operating LCOE. On the other hand, although a decrease in the operating LCOE is obtained by adopting a multi-scenario approach instead of the single-scenario, this reduction becomes more and more marginal with the rise of the storage capacity. This is due to the reduction of the negative effects on the LCOE led by the ORC part-load operations, as confirmed by Figure 8, where a reduction of the red bars are observed for the Case #3 (h_{TES} = 2.5 h) and Case #4 (h_{TES}=5 h).

Table 4 - Optimal ORC design as a function of solar multiple and TES capacity by adopting the single and the multi-scenarios approach (working fluid: Toluene).

Case study	n_s	T_{CD} [°C]	T_{EV} [°C]	ΔT_{SH} [°C]	ε_{REC} [-]	$\dot{m}_{WF}$ [kg/s]	$LCOE_D$ [€/MWh]	$LCOE_{OP}$ [€/MWh]
Case #1 *(SM=1, h_{TES}=0)*	1	49.4	201.1	6.4	-	5.6	91.1	190.2
	3	45.4	204.1	29.5	-	5.0	170.7	179.6
	5	48.1	207.9	27.2	-	5.2	163.7	177.2
	9	45.8	211.2	19.2	-	5.2	172.2	177.0
Case #2 *(SM=1.5, h_{TES}=0)*	1	49.4	201.1	6.4	-	5.6	91.1	134.7
	3	47.4	207.0	28.1	-	5.2	126.4	131.7
	5	47.4	207.0	27.6	-	5.2	124.5	131.4
	9	46.4	213.8	12.2	-	5.3	129.0	131.3
Case #3 *(SM=1.5, h_{TES}=2.5h)*	1	49.4	201.1	6.4	-	5.6	91.1	124.7
	3	47.9	214.3	11.9	-	5.4	118.5	121.4
	5	49.4	220.1	5.5	-	5.4	118.5	121.3
	9	49.2	221.1	4.5	-	5.4	120.5	121.3
Case #4 *(SM=1.5, h_{TES}=5h)*	1	49.4	201.1	6.4	-	5.6	91.1	122.7
	3	47.3	215.0	11.8	-	5.3	116.7	121.1
	5	47.2	214.1	12.7	-	5.3	116.0	121.1
	9	49.1	221.0	1.4	-	5.4	119.2	120.4

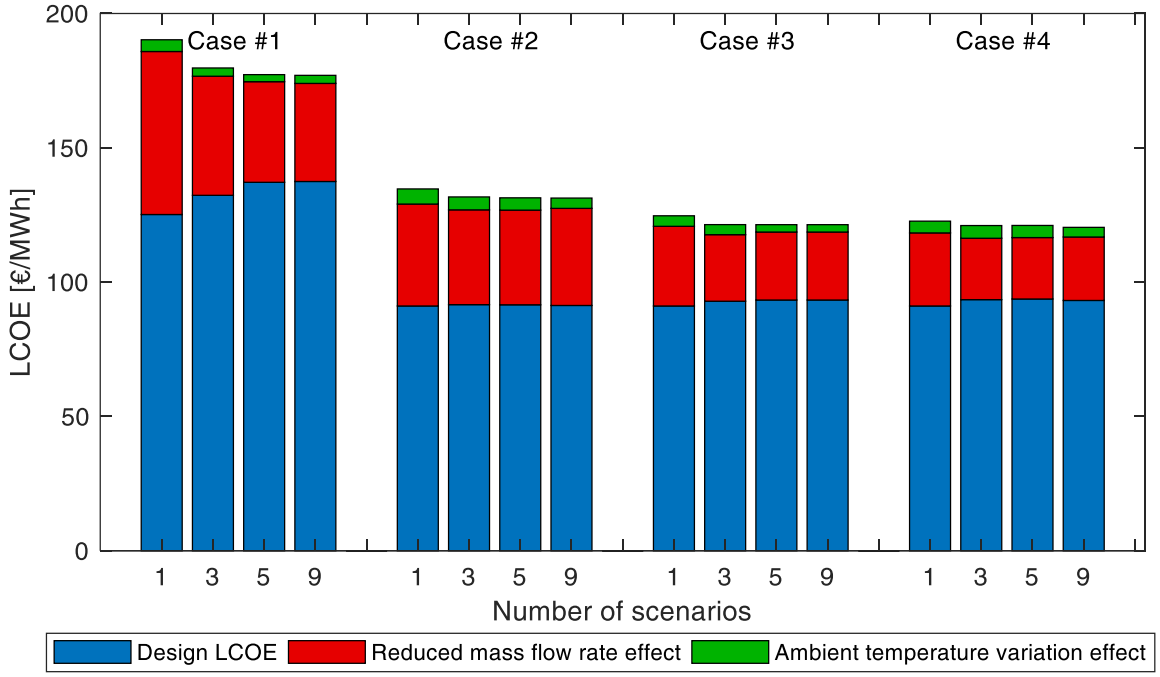

Figure 8 - Levelized cost of energy obtained for different storage capacities using Toluene.

4.2 Computational performance

This last section is dedicated to the influence of the number the scenarios involved in the optimization process on the computational time required to find the minimum LCOE based on the stop criteria assumed. As a figure of comparison, Table 5 reports the average computational times required by the optimization tool performed with a pc Dell XPS8900, CPU Intel Core i7-6700 3.4 GHz, 16 GB RAM. These values should be considered as a qualitative indicator only, since they depend on the model implementation, number of individuals per population, stop criteria and computer performance. Obviously, the higher the number of scenarios is, the larger the required computational effort is. An important spread in the computational time is also observed between the use of a multi-scenario

approach instead of a single-scenario one. For instance, with the involvement of 9 scenarios, on average, more than one day of simulation is required to find the optimum. However, it is worth noting that the proposed method is applied during the design-stage of the ORC unit and not during the real-time operation of the power plant. Therefore, no constraints on the required running times are usually introduced at this stage. Furthermore, the algorithm was not optimized from a computational point of view (in particular during the simulation of the off-design conditions). Obviously, the achievement of reduced computational times will become mandatory with the rise of the number of scenarios involved.

Table 5 – Mean computation times required to find the optimal ORC design configuration

Number of scenarios	Computational time [h]
1	0.8
3	7.5
5	12.1
9	26.2

5. CONCLUSIONS

Although the possibility of exploiting different heat sources for the electricity production makes ORC units a useful and flexible technology, the variations in the heat source and heat sink characteristics during the ORC lifetime could strongly penalize the overall system performance. For this reason, the proper characterization of the heat source and heat sink, including their foreseen variations, could be beneficial even during the ORC design process, leading to more robust design solutions able to achieve better mean performance during the overall plant operation phase. In this framework, the approach for the robust preliminary design of ORC systems proposed by the authors in a previous paper was tested by referring to an ORC unit coupled with a solar field with and without the introduction of a TES system. The variability of the HTF mass flow rate due to fluctuations of the solar radiation, together with the variation in the ambient temperature, are introduced in the design phase through the generation of proper scenarios with a corresponding probability of occurrence and the minimization of the expected LCOE has been set as objective function.
The major outcomes of the study can be highlighted as follows:

- The adoption of a multi-scenario approach leads to an ORC configuration less sensitive to the variation of external parameters and allows to achieve an operating LCOE lower than that obtained with a single-scenario approach;
- The advantages in using a multi-scenario approach instead of a single scenario one are common to all the working fluids examined and becomes more and more evident with the increase of the uncertainty of the input parameter. Important economic benefits could therefore arise from the adoption of the proposed design methodology;
- The rise of the number of scenarios leads to a reduction of the operating LCOE even if requires increasing computational times and the marginal benefits becomes more and more negligible.

ACKNOWLEDGEMENT

This paper is part of the research project funded by P.O.R. SARDEGNA F.S.E. 2014-2020 - Axis III Education and Training, Thematic Goal 10, Specific goal 10.5, Action partnership agreement 10.5.12 – "Call for funding of research projects – Year 2017".

NOMENCLATURE

Symbol		
A	heat transfer area	(m^2)
C_{ANN}	annual costs	(€/year)
C_{IN}	installation costs	(€)
h_{TES}	TES capacity	(h)
LCOE	levelized cost of energy	(€/MWh)

$\dot{m}$	mass flow rate	(kg/s)
n_s	number of scenarios	(-)
p_s	probability of occurrence	(-)
SM	solar multiple	(-)
t_{OP}	ORC operating time	(h)
T	temperature	(°C)
$\dot{W}$	electrical power	(MW)
$\bar{W}_{EXP}$	expected annual energy production	(MWh)
$\bar{W}_{EFF}$	effective annual energy production	(MWh)
Δh	specific enthalpy change	(kJ/kg)
ε	heat exchanger effectiveness	(-)
η	efficiency	(-)

Subscript

CD	condenser
D	design conditions
EV	evaporator
EM	electro-mechanical
HTF	heat transfer fluid
OP	operating conditions
P	pump
REC	recuperator
SH	superheating
T	turbine
WF	working fluid

REFERENCES

[1] E. Macchi, M. Astolfi, Organic Rankine Cycle Power Systems, 2017.

[2] S. Quoilin, M. Van Den Broek, S. Declaye, P. Dewallef, V. Lemort, Techno-economic survey of Organic Rankine Cycle (ORC) systems, Renew. Sustain. Energy Rev. 22 (2013) 168–186. https://doi.org/10.1016/j.rser.2013.01.028.

[3] V. Pethurajan, S. Sivan, G.C. Joy, Issues, comparisons, turbine selections and applications – An overview in organic Rankine cycle, Energy Convers. Manag. 166 (2018) 474–488. https://doi.org/10.1016/J.ENCONMAN.2018.04.058.

[4] V.R. Patil, V.I. Biradar, R. Shreyas, P. Garg, M.S. Orosz, N.C. Thirumalai, Techno-economic comparison of solar organic Rankine cycle (ORC) and photovoltaic (PV) systems with energy storage, Renew. Energy. 113 (2017) 1250–1260. https://doi.org/10.1016/j.renene.2017.06.107.

[5] M. Petrollese, G. Cau, D. Cocco, The Ottana solar facility: dispatchable power from small-scale CSP plants based on ORC systems, Renew. Energy. 147 (2020) 2932–2943. https://doi.org/10.1016/j.renene.2018.07.013.

[6] O. Aboelwafa, S.-E.K. Fateen, A. Soliman, I.M. Ismail, A review on solar Rankine cycles: Working fluids, applications, and cycle modifications, Renew. Sustain. Energy Rev. 82 (2018) 868–885. https://doi.org/10.1016/j.rser.2017.09.097.

[7] L. Liu, T. Zhu, J. Ma, Working fluid charge oriented off-design modeling of a small scale Organic Rankine Cycle system, Energy Convers. Manag. 148 (2017) 944–953. https://doi.org/10.1016/J.ENCONMAN.2017.06.009.

[8] Y.-L. He, D.-H. Mei, W.-Q. Tao, W.-W. Yang, H.-L. Liu, Simulation of the parabolic trough solar energy generation system with Organic Rankine Cycle, Appl. Energy. 97 (2012) 630–641. https://doi.org/10.1016/j.apenergy.2012.02.047.

[9] J. Wang, Z. Yan, P. Zhao, Y. Dai, G.W. Woodruff, Off-design performance analysis of a solar-powered organic Rankine cycle, Energy Convers. Manag. 80 (2014) 150–157. https://doi.org/10.1016/j.enconman.2014.01.032.

[10] F. Calise, C. Capuozzo, A. Carotenuto, L. Vanoli, Thermoeconomic analysis and off-design performance of an organic Rankine cycle powered by medium-temperature heat sources, Sol. Energy. 103 (2014) 595–609. https://doi.org/10.1016/j.solener.2013.09.031.
[11] S. Li, H. Ma, W. Li, Dynamic performance analysis of solar organic Rankine cycle with thermal energy storage, Appl. Therm. Eng. 129 (2018) 155–164. https://doi.org/10.1016/j.applthermaleng.2017.10.021.
[12] L. Cioccolanti, R. Tascioni, A. Arteconi, Mathematical modelling of operation modes and performance evaluation of an innovative small-scale concentrated solar organic Rankine cycle plant, Appl. Energy. 221 (2018) 464–476. https://doi.org/10.1016/j.apenergy.2018.03.189.
[13] M. Usman, M. Imran, Y. Yang, D.H. Lee, B.-S. Park, Thermo-economic comparison of air-cooled and cooling tower based Organic Rankine Cycle (ORC) with R245fa and R1233zde as candidate working fluids for different geographical climate conditions, Energy. 123 (2017) 353–366. https://doi.org/10.1016/j.energy.2017.01.134.
[14] R. Dickes, O. Dumont, R. Daccord, S. Quoilin, V. Lemort, Modelling of organic Rankine cycle power systems in off-design conditions: An experimentally-validated comparative study, Energy. 123 (2017) 710–727. https://doi.org/10.1016/j.energy.2017.01.130.
[15] E.W. Law, A.A. Prasad, M. Kay, R.A. Taylor, Direct normal irradiance forecasting and its application to concentrated solar thermal output forecasting - A review, Sol. Energy. 108 (2014) 287–307. https://doi.org/10.1016/j.solener.2014.07.008.
[16] H. Hajabdollahi, A. Ganjehkaviri, M. Nazri, M. Jaafar, Thermo-economic optimization of RSORC (regenerative solar organic Rankine cycle) considering hourly analysis, Energy. 87 (2015) 369–380. https://doi.org/10.1016/j.energy.2015.04.113.
[17] P. Mavrou, A.I. Papadopoulos, P. Seferlis, P. Linke, S. Voutetakis, Selection of working fluid mixtures for flexible Organic Rankine Cycles under operating variability through a systematic nonlinear sensitivity analysis approach, Appl. Therm. Eng. 89 (2015) 1054–1067. https://doi.org/10.1016/j.applthermaleng.2015.06.017.
[18] E.A. Bufi, S.M. Camporeale, P. Cinnella, Robust optimization of an Organic Rankine Cycle for heavy duty engine waste heat recovery, Energy Procedia. 129 (2017) 66–73. https://doi.org/10.1016/j.egypro.2017.09.190.
[19] S. Van Erdeweghe, J. Van Bael, B. Laenen, W. D'haeseleer, Design and off-design optimization procedure for low-temperature geothermal organic Rankine cycles, Appl. Energy. 242 (2019) 716–731. https://doi.org/10.1016/J.APENERGY.2019.03.142.
[20] R. Pili, A. Romagnoli, M. Jiménez-Arreola, H. Spliethoff, C. Wieland, Simulation of Organic Rankine Cycle – Quasi-steady state vs dynamic approach for optimal economic performance, Energy. 167 (2019) 619–640. https://doi.org/10.1016/j.energy.2018.10.166.
[21] M. Petrollese, D. Cocco, Robust optimization for the preliminary design of solar organic Rankine cycle (ORC) systems, Energy Convers. Manag. 184 (2019) 338–349. https://doi.org/10.1016/j.enconman.2019.01.060.
[22] I.H. Bell, J. Wronski, S. Quoilin, V. Lemort, Pure and Pseudo-pure Fluid Thermophysical Property Evaluation and the Open-Source Thermophysical Property Library CoolProp, Ind. Eng. Chem. Res. 53 (2014) 2498–2508. https://doi.org/10.1021/ie4033999.
[23] S.G. Kandlikar, Development of a Flow Boiling Map for Subcooled and Saturated Flow Boiling of Different Fluids Inside Circular Tubes, J. Heat Transfer. 113 (1991) 190–200. http://dx.doi.org/10.1115/1.2910524.
[24] S.G. Kandlikar, Handbook of phase change: boiling and condensation, CRC Press, Philadelphia, USA, 1999.
[25] M. Astolfi, E. Macchi, Efficiency Correlations for Axial Flow Turbines Working With Non-Conventional Fluids, in: 3rd Int. Semin. ORC Power Syst., Brussels, Belgium, 2015: pp. 1–12. https://doi.org/10.1115/1.3230794.
[26] R. Gabbrielli, A novel design approach for small scale low enthalpy binary geothermal power plants, Energy Convers. Manag. 64 (2012) 263–272. https://doi.org/10.1016/j.enconman.2012.04.017.
[27] R. Turton, R. Bailie, W. Whiting, J. Shaeiwitz, Analysis, synthesis and design of chemical processes, Third Edit, Pearson Education, Upper Saddle River, N.J., USA, 2008.
[28] D. Cocco, L. Migliari, M. Petrollese, A hybrid CSP–CPV system for improving the

dispatchability of solar power plants, Energy Convers. Manag. 114 (2016) 312–323. https://doi.org/10.1016/j.enconman.2016.02.015.